

Article

Paper Electrodes Coated with Partially-Exfoliated Graphite and Polypyrrole for High-Performance Flexible Supercapacitors

Leping Huang ¹, Weida Rao ¹, Lingling Fan ², Jie Xu ^{1,*}, Zikui Bai ¹, Weilin Xu ^{1,2}
and Haifeng Bao ^{1,*}

¹ State Key Laboratory for Hubei New Textile Materials and Advanced Processing Technology, School of Materials Science & Engineering, Wuhan Textile University, Wuhan 430200, China; hlp71@126.com (L.H.); weidayumiko@163.com (W.R.); zkbwn@163.com (Z.B.); weilin-xu@hotmail.com (W.X.)

² School of Textile Science & Engineering, Wuhan Textile University, Wuhan 430200, China; hglingling@126.com

* Correspondence: xujie0@ustc.edu (J.X.); baohaifeng@wtu.edu.cn (H.B.)

Received: 11 December 2017; Accepted: 25 January 2018; Published: 31 January 2018

Abstract: Flexible paper electrodes for supercapacitors were prepared with partially-exfoliated graphite and polypyrrole as the active materials. Graphite was coated on paper with pencil drawing and then electrochemically exfoliated using the cyclic voltammetry (CV) technique to obtain the exfoliated graphite (EG)-coated paper (EG-paper). Polypyrrole (PPy) doped with β -naphthalene sulfonate anions was deposited on EG-paper through in-situ polymerization, leading to the formation of PPy-EG-paper. The as-prepared PPy-EG-paper showed a high electrical conductivity of $10.0 \text{ S}\cdot\text{cm}^{-1}$ and could be directly used as supercapacitor electrodes. The PPy-EG-paper electrodes gave a remarkably larger specific capacitance of $2148 \text{ F}\cdot\text{g}^{-1}$ at a current density of $0.8 \text{ mA}\cdot\text{cm}^{-2}$, compared to PPy-graphite-paper ($848 \text{ F}\cdot\text{g}^{-1}$). The capacitance value of PPy-EG-paper could be preserved by 80.4% after 1000 charge/discharge cycles. In addition, the PPy-EG-paper electrodes demonstrated a good rate capability and a high energy density of $110.3 \text{ Wh}\cdot\text{kg}^{-1}$ at a power density of $121.9 \text{ W}\cdot\text{kg}^{-1}$. This work will pave the way for the discovery of efficient paper-based electrode materials.

Keywords: paper; polypyrrole; partially-exfoliated graphite; supercapacitor

1. Introduction

Flexible electronics have recently attracted considerable attention because of their potential applications in rollable displays, e-paper, smart textiles, distributed sensors, radio frequency identification, embedded health monitoring devices, and so on [1–6]. As an important component to power the functional devices, there is a crucial challenge to develop lightweight, flexible, and high-performance energy storage devices [6–8]. Flexible supercapacitors have been one of the most promising energy storage devices due to their high power density, long cycle life, and fast charge-discharge rate [9]. Based on the energy storage mechanisms, supercapacitors can be divided into two main types, namely electrical double-layer capacitors (EDLCs) and pseudocapacitors. EDLCs are electrostatic storage of the electrical energy done by separating the charge in a double layer at the interface between electrode and electrolyte, while pseudocapacitors provide electrochemical storage of the electrical energy, achieved by faradic redox reactions.

Polypyrrole (PPy), a representative conducting polymer, was widely used as a pseudocapacitive electrode material due to its low cost, high theoretical specific capacitance, superior electrical conductivity, fast redox activity, appreciable mechanical property, and facile preparation [10–21]. However, most

PPy-based electrodes retain less than 50% of the initial capacitance after 1000 charge/discharge cycles [22], which is not acceptable for supercapacitors. The charge/discharge cycling instability of PPy is mainly due to structural deformation and counter-ion drain effect [23]. The backbone of the PPy chains experiences repeated swelling and shrinking during cycling as a result of doping and dedoping of counter-ions, leading to structural pulverization and, thus, fast capacitance decay. Moreover, some of the ion channels collapse when anions diffuse back to the electrolyte, making anions more difficult to re-dope the PPy backbone. Thus, the conductivity and capacitance of PPy would reduce slowly. Extensive efforts have been devoted to improve the cycling stability of PPy, including integrating PPy into flexible substrates, such as graphene [24] and carbon nanotubes (CNTs) [25], and doping PPy with special anionic dopants [23,26,27].

Paper, as one of the most available flexible products, is not only used for information recording and packaging, but has also been considered as a promising flexible substrate for energy storage devices due to its wide availability, low cost, light weight, environmental friendliness, recyclability, and bendability [6,28]. Zheng et al. used a pure graphite rod to draw on Xerox cellulose paper to obtain a solvent-free drawing electrode [29]. An aqueous supercapacitor based on the pencil-drawing paper electrodes can deliver a specific capacitance of $12 \text{ F}\cdot\text{g}^{-1}$ at a current density of $10 \text{ mA}\cdot\text{g}^{-1}$ and retain 90% its initial capacitance after 15,000 cycles. The device displays excellent cycling stability; however, its specific capacitance is still relatively low. Later, Tao et al. used an electrochemical deposition method to grow PPy on the pencil-drawing graphite paper [30]. A solid-state supercapacitor fabricated with the PPy/graphite coated paper achieved a high volumetric specific capacitance of $52.9 \text{ F}\cdot\text{cm}^{-3}$ at a scan rate of $1 \text{ mV}\cdot\text{s}^{-1}$.

Functionalized exfoliated graphite (EG) has been demonstrated to offer a large surface area for supporting pseudo-capacitive materials [31]. The strong attachment of functionalized graphene on the graphite base could minimize the interfacial contact resistance and, thus, improve the rate capability of pseudo-capacitive electrodes. In this work, we prepared flexible paper electrodes coated with EG and PPy. Graphite was coated on paper with pencil drawing and then electrochemically exfoliated to obtain the EG coated paper (EG-paper). Polypyrrole (PPy) doped with β -naphthalene sulfonate anions was deposited on EG-paper. The as-prepared PPy-EG-paper electrode delivered an enhanced specific capacitance, superior cycling stability, and good rate capability, thereby making it a viable electrode material for flexible supercapacitors.

2. Materials and Methods

2.1. Materials

Pyrrrole, cetyltrimethylammonium bromide (CTAB), sodium dodecyl benzene sulfonate (SDBS), β -naphthalene sulfonic acid, and other chemicals were purchased from Sinopharm Chemical Reagent Co., Ltd. (Shanghai, China) and used as received. Deionized water ($18.2 \text{ M}\Omega\cdot\text{cm}^{-1}$) was obtained from a Milli-Q water-purification system.

2.2. Preparation of PPy-EG-paper

A piece of Sketch paper (Maxleaf, Jianli, China) with an area of about 2.0 cm^2 was drawn with a 4B pencil (Zhonghua, Shanghai, China) 50 times to form a continuous graphite layer onto the paper. Pencil drawing provides a rapid and extremely cost-effective approach for the production of electrochemical platforms. However, the number of layers affects the electrochemical signal dramatically [32,33]. The graphite layer could be screen-printed on the paper by using graphite paste for repeatability and reproducibility. The graphite-coated paper (G-paper) was used as the working electrode in a three-electrode electrochemical system with saturated calomel electrode (SCE) as the reference electrode and platinum (Pt) foil as the counter electrode. The G-paper electrode was scanned on an Autolab PGSTAT302N potentiostat/galvanostat system (Metrohm AG, Herisau, Switzerland) for six cycles between 0.5 and 1.8 V versus SCE at a scan rate of $20 \text{ mV}\cdot\text{s}^{-1}$ in $0.5 \text{ M K}_2\text{CO}_3$ aqueous solution.

The G-paper electrode was then further scanned for another ten cycles between -1.0 and 1.9 V versus SCE at $20 \text{ mV}\cdot\text{s}^{-1}$ in phosphate-buffered saline containing 1 M KNO_3 ($\text{pH} = 6.7$). In each cycle, the G-paper electrode was kept at 1.9 V versus SCE for 5 s . The paper was cleaned with deionized water and ethanol and vacuum-dried at ambient temperature. Thus, the exfoliated graphite-coated paper (EG-paper) was obtained.

PPy was deposited on the EG-paper via in-situ polymerization as previously reported [13–15]. Briefly, the EG-paper was dipped into 100 mL aqueous solution containing pyrrole (1.0 M), CTAB (0.002 M), and SDBS (0.002 M) and stirred for 30 min . Then, 100 mL aqueous solution of FeCl_3 (0.5 M) was slowly added to the mixture under stirring. The mixture was stirred for another 2 h at $5 \text{ }^\circ\text{C}$. The resulting paper was then immersed in 0.5 M aqueous solution of β -naphthalene sulfonic acid for 30 min . The paper was brought out and washed with deionized water and ethanol, in sequence, three times. Finally, the paper was dried at $60 \text{ }^\circ\text{C}$ overnight. The thus-obtained PPy-coated EG-paper was denoted as PPy-EG-paper.

For comparison, the PPy-coated G-paper (denoted as PPy-G-paper) was also prepared according to the same procedure using the G-paper substrate as a control sample.

2.3. Characterization

Scanning electron microscopy (SEM, JEOL JSM-6510LV, Tokyo, Japan, operated at 10 kV) was used to investigate the morphology. Raman spectra were obtained with a Renishaw microRaman spectroscopy system (633 nm , Renishaw, Derbyshire, UK). The Brunauer–Emmett–Teller (BET) surface area was measured on a TriStar II 3020 analyzer (Micromeritics Instrument Corp., Norcross, GA, USA). Attenuated total reflection Fourier transformed infrared (ATR-FTIR) spectra were recorded on a Tensor 27 (Bruker, Ettlingen, Germany) in the range of $4000\text{--}600 \text{ cm}^{-1}$. Surface conductivity was determined on a digital four-point probe resistivity measurement system (RTS-9, Probes Tech. Co., Shenzhen, China).

Electrochemical measurements were carried out via a two-electrode symmetric supercapacitor system. The sample and mass of positive and negative electrodes are exactly the same. The coated paper was directly used as the electrodes, and the electrolyte was a 2.0 M NaCl aqueous solution. Cyclic voltammetry (CV) curves were collected within the voltage range of $-0.9\text{--}+0.9 \text{ V}$ at various scan rates (5 to $100 \text{ mV}\cdot\text{s}^{-1}$) on an Autolab PGSTAT302N. Galvanostatic charge-discharge (GCD) cycling measurements were conducted over the potential range from 0 to 0.8 V on a multichannel LAND CT2001A battery testing device (Wuhan Land Electronics, Wuhan, China). The mass of the active material was determined by weight measurements before and after the coating of the active material.

3. Results and Discussion

The fabrication process of the PPy-EG-paper composite is illustrated in Figure 1a. The white paper blackened after the pencil drawing and turned black completely after the PPy deposition (Figure 1b). The paper mainly consists of cellulose fibers (Figure 2a). It can be seen from Figure 2b that the lamellar graphite was produced and coated on the paper substrate with pencil drawing. The graphite was partially electrochemically exfoliated using the CV method and the graphene multilayers were formed in small sizes (dimensions of one to a few microns, Figure 2c). The BET surface area of EG-paper was about $3.91 \text{ m}^2/\text{g}$, which is higher than that of G-paper ($3.01 \text{ m}^2/\text{g}$). The enlarged surface area could support the deposition of PPy. The structure of EG could maintain the electronic connections between graphene sheets through the graphite matrix, which will facilitate electron transfer and benefit electrochemical reactions [34]. After in situ polymerization, PPy was successfully wrapped on the G-paper and EG-paper (Figure 2d,e). The PPy coatings were agglomerated into lumps with different sizes. The PPy particles in the PPy-EG-paper composites were smaller in size and more regular in shape as compared with those in the PPy-G-paper. The PPy particles were stacked to form a three-dimensional interconnected network, which could be beneficial to enhance the electrolyte adsorption and expand the ion transport channels.

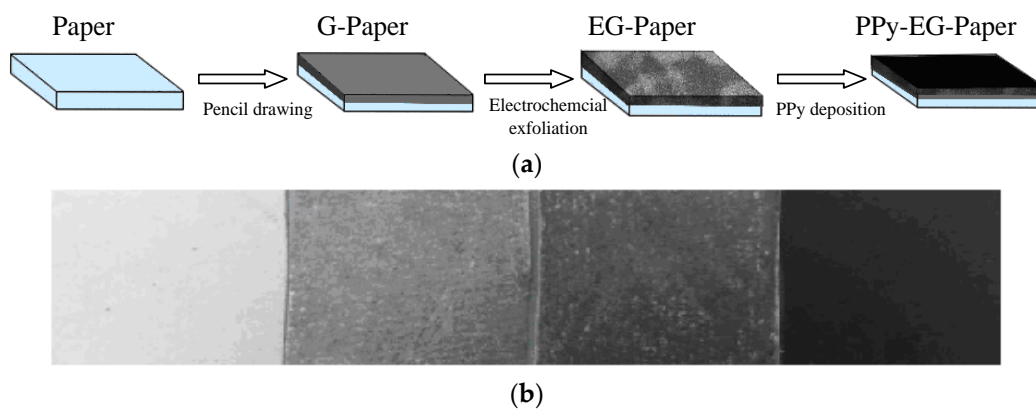


Figure 1. (a) Schematic of fabrication process of the PPy-EG-paper; and (b) photographs of the blank paper, G-paper, EG-paper, and PPy-EG-paper.

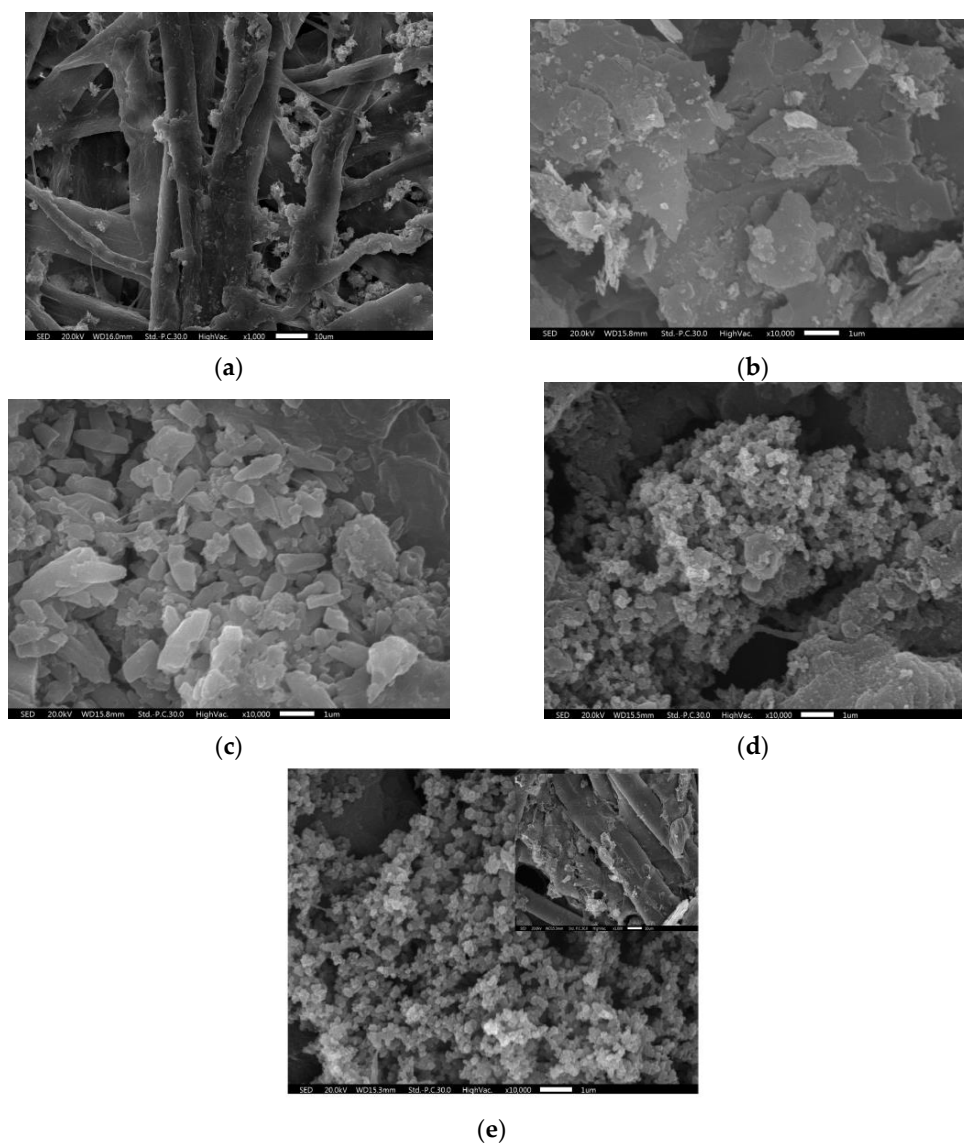


Figure 2. SEM images of (a) blank paper; (b) G-paper; (c) EG-paper; (d) PPy-G-paper; and (e) PPy-EG-paper.

The mass loading of PPy of the total weight of the composite paper was about 9.5% and 6.5% for PPy-G-paper and PPy-EG-paper, respectively. The electrical conductivity was about 3.3 and 10.0 S·cm⁻¹ for PPy-G-paper and PPy-EG-paper, respectively. The conductivity of PPy-EG-paper is higher than those of PPy-coated Cladophora paper (about 1 S·cm⁻¹) [35], PPy/MWCNTs/bacterial cellulose (BC) composite paper (7.78 S·cm⁻¹) [36], PPy/BC paper (3.9 S·cm⁻¹) [12], and pure PPy (1.14 S·cm⁻¹) [37]. In order to demonstrate the suitability of PPy-EG-paper for flexible electrode materials, the conductance stability of PPy-EG-paper at different curvatures (Figure 3) was measured by monitoring the current at a fixed voltage of 0.8 V. It can be observed that the current was nearly unchanged at different bending states, revealing that the conductance of PPy-EG-paper is hardly affected by bending stress and, thus, confirming its promising potential in flexible electronics.

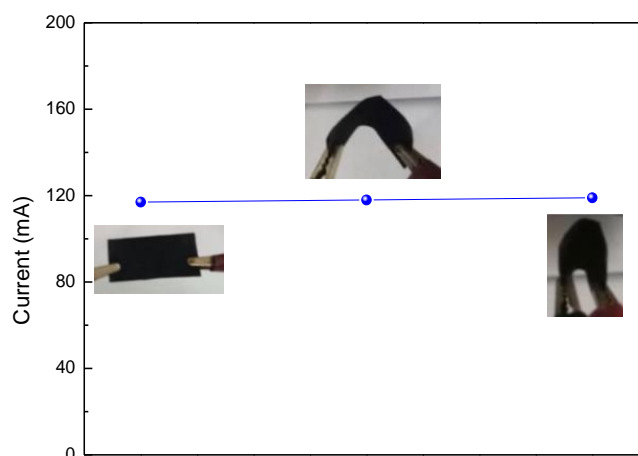


Figure 3. The current PPy-EG-paper bent with different curvatures under a constant voltage of 0.8 V.

Raman spectra of G-paper and EG-paper are shown in Figure 4a. For both G-paper and EG-paper, the spectra exhibited the D (1346 cm⁻¹) and G (1579 cm⁻¹) bands. The D band represents the breathing vibration modes of sp² carbon atoms. The G band represents the in-plane vibration modes of sp² carbon atoms. The relative intensity of the D to G bands for EG-paper was larger than that for G-paper, confirming the exfoliation of graphite. The blank paper, EG-paper, and PPy-EG-paper were characterized by ATR-FTIR and the results are shown in Figure 4b. The spectrum of the blank paper was featured by the typical overlapping bands of the functional groups (C–O, C–C, and C–O–C) of cellulose at 1157, 1103, and 1022 cm⁻¹. These bands disappeared for EG-paper due to the coating of EG. In the case of PPy-EG-paper, the main peaks corresponding to PPy [38,39] could be observed. The band between 1550 and 1460 cm⁻¹ was due to the C=C stretching vibration in pyrrole ring. The C–N stretching vibration was located at 1378 cm⁻¹. The band at 1250 cm⁻¹ was assigned to the C–H and C–N in-plane deformation vibrations. The C–H bending vibration was located at 1111 cm⁻¹. The peak at 1077 cm⁻¹ was attributed to the in-plane deformation vibration of NH₂⁺ groups in the protonated PPy chains. The N–H in-plane deformation vibration band was found at 985 cm⁻¹.

To investigate the electrochemical properties of the as-prepared PPy-EG-paper, symmetrical supercapacitor devices were fabricated and subjected to CV measurements in a voltage window of −0.9–+0.9 V using a NaCl aqueous electrolyte. The CV curves of EG-paper, PPy-G-paper, and PPy-EG-paper with a scan rate of 5 mV·s⁻¹ are shown in Figure 5. Notably, the current densities of PPy-G-paper and PPy-EG-paper were significantly larger than that of EG-paper, indicating a significant contribution of pseudocapacitance by PPy. Both the CV curves of PPy-G-paper and PPy-EG-paper exhibited a quasi-rectangular shape without obvious redox peaks, implying their good capacitive behavior. Furthermore, PPy-EG-paper possessed the larger enclosed area on the CV curve than PPy-G-paper, demonstrating higher specific capacitance.

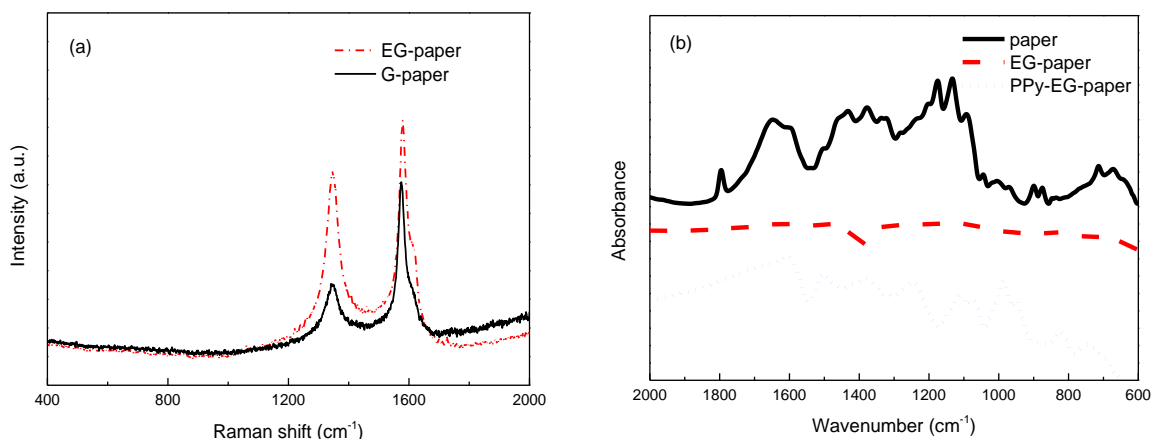


Figure 4. (a) Raman spectra of G-paper and EG-paper; and (b) FTIR spectra of the blank paper, EG-paper, PPy-EG-paper.

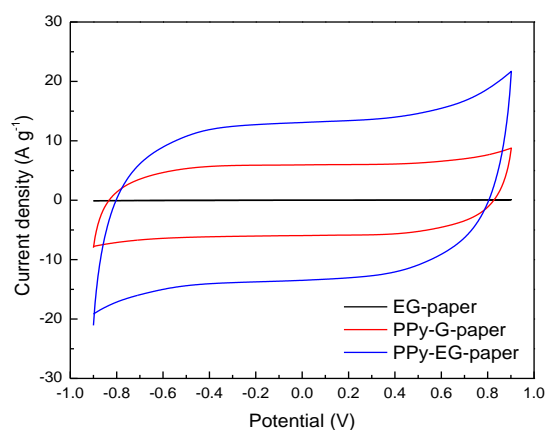


Figure 5. CV curves of EG-paper, PPy-G-paper, and PPy-EG-paper at a scan rate of $5 \text{ mV}\cdot\text{s}^{-1}$.

The CV curves of PPy-G-paper and PPy-EG-paper with different scan rates ranging from 5 to $100 \text{ mV}\cdot\text{s}^{-1}$ are shown in Figure 6a,b. The shape of the CV curves gradually transformed from a distorted rectangle to an oval upon increasing the scan rate. This may be attributed to the inhibition of charge collection by the internal resistance of the electrode and the diffusion limitations of Na^+ in the inner active surfaces of the electrode [40]. The mass-specific capacitance can be calculated from the CV curves using the following equation:

$$C_{sp} = \frac{\int IdV}{f \times \Delta V \times m}$$

where I is the current, V is the voltage, f is the scan rate of the CV curves, ΔV is the whole voltage difference, and m is the mass of the electroactive material. The obtained mass-specific capacitances as a function of the scan rate for PPy-G-paper and PPy-EG-paper are shown in Figure 6c. The specific capacitance of PPy-G-paper and PPy-EG-paper was calculated from the CV curves to be 1347 and $2253 \text{ F}\cdot\text{g}^{-1}$, respectively, at a low scan rate of $5 \text{ mV}\cdot\text{s}^{-1}$. It can be found that the capacitance of PPy-G-paper and PPy-EG-paper was decreased as the scan rates increased, which is explained by the ion diffusion effect in the electrode materials and at the electrode/electrolyte interface [41]. Interestingly, even at a high sweep rate of $50 \text{ mV}\cdot\text{s}^{-1}$, the capacitance of PPy-EG-paper remained relatively high (i.e., $1073 \text{ F}\cdot\text{g}^{-1}$). It is obvious that the capacitance of PPy-EG-paper was higher than that of PPy-G-paper at all scan rates. These results indicate that PPy-EG-paper exhibited a good rate capability upon increasing the scan rate. Furthermore, the specific capacitance values of

PPy-EG-paper are significantly higher than those of other recently-reported paper electrodes, such as $\text{MnO}_2/\text{Ni}/\text{graphite}/\text{paper}$ ($680 \text{ F}\cdot\text{g}^{-1}$ at $5 \text{ mV}\cdot\text{s}^{-1}$) [42], $\text{Mn}_3\text{O}_4/\text{Ni}/\text{graphite}/\text{paper}$ ($432 \text{ F}\cdot\text{g}^{-1}$ at $5 \text{ mV}\cdot\text{s}^{-1}$) [43], $\text{PANI}/\text{nylon}/\text{cellulose acetate}$ ($400 \text{ F}\cdot\text{g}^{-1}$ at $5 \text{ mV}\cdot\text{s}^{-1}$) [44], $\text{CNTs}/\text{MnO}_2/\text{CNTs}/\text{paper}$ ($327 \text{ F}\cdot\text{g}^{-1}$ at $10 \text{ mV}\cdot\text{s}^{-1}$) [45], and $\text{MnO}_2/\text{MWCNTs}/\text{paper}$ ($1035 \text{ F}\cdot\text{g}^{-1}$ at $2 \text{ mV}\cdot\text{s}^{-1}$) [46].

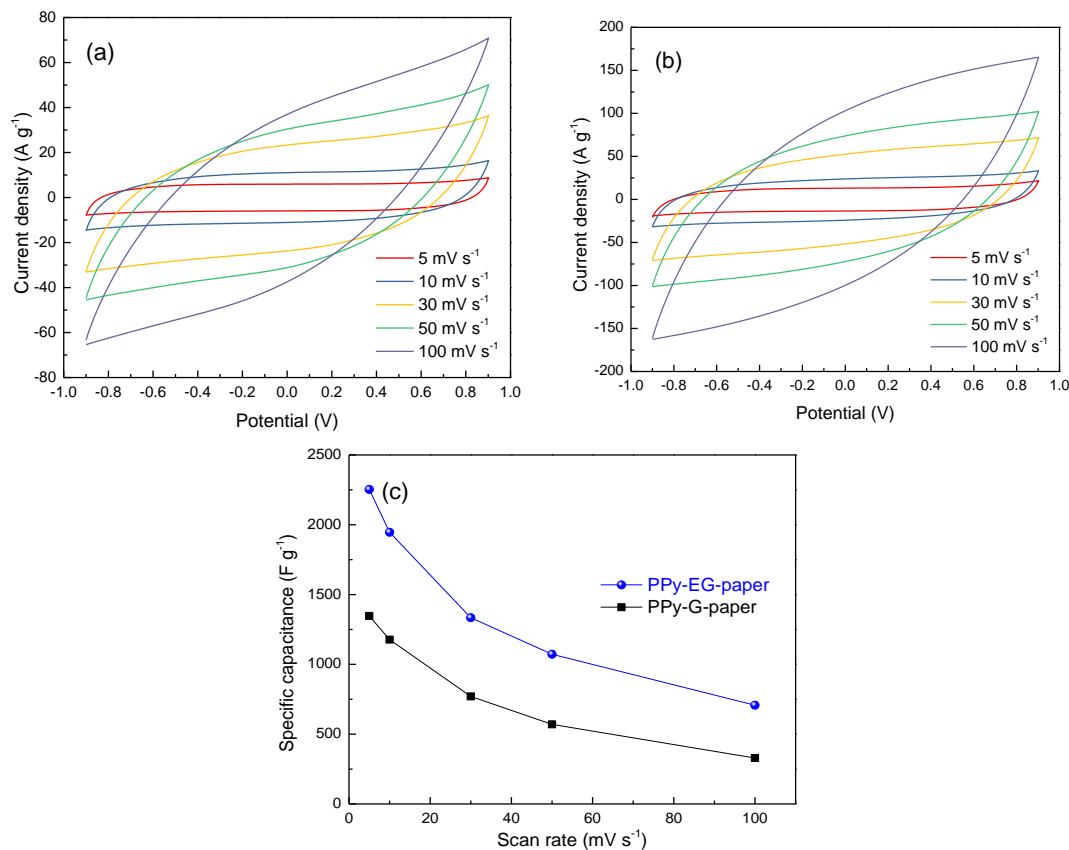


Figure 6. CV curves of (a) PPy-G-paper and (b) PPy-EG-paper at different scan rates; and (c) specific capacitance of PPy-G-paper and PPy-EG-paper at different scan rates.

The GCD curves of PPy-G-paper and PPy-EG-paper at the same current density of $0.8 \text{ mA}\cdot\text{cm}^{-2}$ are illustrated in Figure 7a. The curve of PPy-EG-paper had symmetrical triangle and small internal resistance drop (IR_{drop}), demonstrating the superior reversibility of charging/discharging. The equivalent series resistance due to electrolyte resistance, electrode resistance, and contact resistance might be responsible for this IR_{drop} . The IR_{drop} of PPy-EG-paper was lower than that of PPy-G-paper, which is in agreement with the conductivity results. Electrochemical impedance spectroscopy (EIS) was used to further understand the interfacial resistance for PPy-EG-paper and PPy-G-paper. The Nyquist plots are displayed in Figure 7b. The equivalent resistance for PPy-EG-paper was smaller than that for PPy-G-paper, indicating the superior performance of PPy-EG-paper. The specific capacitance (C_m) could be determined based on the GCD profile using the following formula:

$$C_m = \frac{I \times t}{(\Delta V - IR_{drop}) \times m}$$

where I is the discharge current, t is the time elapsed for the discharge from 0 to 0.8 V, ΔV is the voltage difference within the discharge time, IR_{drop} is the IR voltage drop, and m is the mass of the active materials on the electrode. The specific capacitance at $0.8 \text{ mA}\cdot\text{cm}^{-2}$ was calculated to be about 848 and $2148 \text{ F}\cdot\text{g}^{-1}$ for PPy-G-paper and PPy-EG-paper, respectively. The specific capacitance of PPy-EG-paper was significantly higher than that of PPy-G-paper, which is in agreement

with the trend revealed by the CV curves. This value is even higher than the proposed results of PPy-coated paper electrodes ($370 \text{ F}\cdot\text{g}^{-1}$ at $1 \text{ mA}\cdot\text{cm}^{-2}$) [47], PANI/Au/paper electrodes ($560 \text{ F}\cdot\text{g}^{-1}$ at $1.0 \text{ A}\cdot\text{g}^{-1}$) [48], graphene nanosheet/cellulose composite paper electrodes ($252 \text{ F}\cdot\text{g}^{-1}$ at $1 \text{ A}\cdot\text{g}^{-1}$) [49], PANI/cellulose paper electrodes ($160 \text{ F}\cdot\text{g}^{-1}$ at $0.1 \text{ A}\cdot\text{g}^{-1}$) [28], N/S-codoped graphene paper electrodes ($281 \text{ F}\cdot\text{g}^{-1}$ at $1 \text{ A}\cdot\text{g}^{-1}$) [50], $\text{Mn}_3\text{O}_4/\text{Ni}/\text{graphite}/\text{paper}$ electrodes ($372.5 \text{ F}\cdot\text{g}^{-1}$ at $1.0 \text{ mA}\cdot\text{cm}^{-2}$) [43], and PANI/nylon/cellulose acetate ($402 \text{ F}\cdot\text{g}^{-1}$ at $0.3 \text{ A}\cdot\text{g}^{-1}$) [44]. The GCD curves and C_m values for PPy-G-paper and PPy-EG-paper at different current densities are shown in Figure 8a–c. No obvious IR_{drop} appeared with increasing the current density for PPy-EG-paper, indicating its lower resistance. It can be found that the C_m values decreased slightly with the increase of the current densities. When the current density rose up to $6.4 \text{ mA}\cdot\text{cm}^{-2}$, the specific capacitance of PPy-G-paper and PPy-EG-paper remained at 659 and $1669 \text{ F}\cdot\text{g}^{-1}$, respectively, corresponding to 66.3% and 77.8% of the initial values. Specific energy density (E) and power density (P) are calculated using the following equations:

$$E = (1/2)CV^2$$

$$P = E/t$$

where C is the specific capacitance, V the operating voltage and t the discharge time. The Ragone plots of specific power density against specific energy density for PPy-G-paper and PPy-EG-paper are shown in Figure 8d. In both cases, the obtained curves indicate that the specific power density decreased upon increasing the specific energy density. PPy-G-paper showed relatively smaller specific energy and power densities due to the lower C_m values and larger IR drops during the GCD process. In the case of PPy-EG-paper, the energy density reached to about $110.3 \text{ Wh}\cdot\text{kg}^{-1}$ at a power density of $121.9 \text{ W}\cdot\text{kg}^{-1}$, which is remarkably higher than the reported values for paper electrodes, such as PPy-cladophora cellulose paper ($1.75 \text{ Wh}\cdot\text{kg}^{-1}$) [35], nitrogen/sulfur-codoped graphene paper ($28.44 \text{ Wh}\cdot\text{kg}^{-1}$) [50], V_2O_5 -graphene paper (8.5 and $13.3 \text{ Wh}\cdot\text{kg}^{-1}$) [51,52], T- Nb_2O_5 -graphene paper ($47 \text{ Wh}\cdot\text{kg}^{-1}$) [53], V_2O_5 -carbon fiber paper ($45 \text{ Wh}\cdot\text{kg}^{-1}$) [54], and CNT-paper ($48.86 \text{ Wh}\cdot\text{kg}^{-1}$) [55].

Cycling life was used to comprehensively evaluate the electrochemical performance of the electrode materials. Figure 9 displays the cycling stability of PPy-G-paper and PPy-EG-paper at a current density of $0.8 \text{ mA}\cdot\text{cm}^{-2}$. Notably, the downward trend of the specific capacitance for PPy-EG-paper was flat, while the specific capacitance of PPy-G-paper was sharply decreased. After 1000 cycles, the specific capacitance of PPy-EG-paper still possessed $1726 \text{ F}\cdot\text{g}^{-1}$, meaning that 80.4% of its initial value was retained; however, PPy-G-paper would lessen to 54.0% . PPy-EG-paper was endowed with a long cycling life and further stable electrochemical performance. Thus, the above results indicate that the PPy-EG-paper electrodes prepared herein exhibited high specific capacitance, low ESRs, good capacitance retention, and good cycling stabilities, revealing their great potential for flexible energy storage.

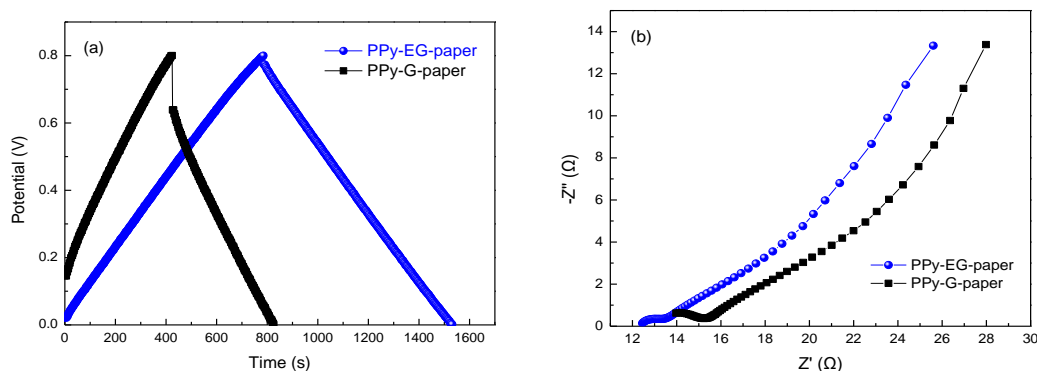


Figure 7. (a) GCD curves of PPy-G-paper and PPy-EG-paper at a current density of $0.8 \text{ mA}\cdot\text{cm}^{-2}$; and (b) Nyquist plots of PPy-G-paper and PPy-EG-paper.

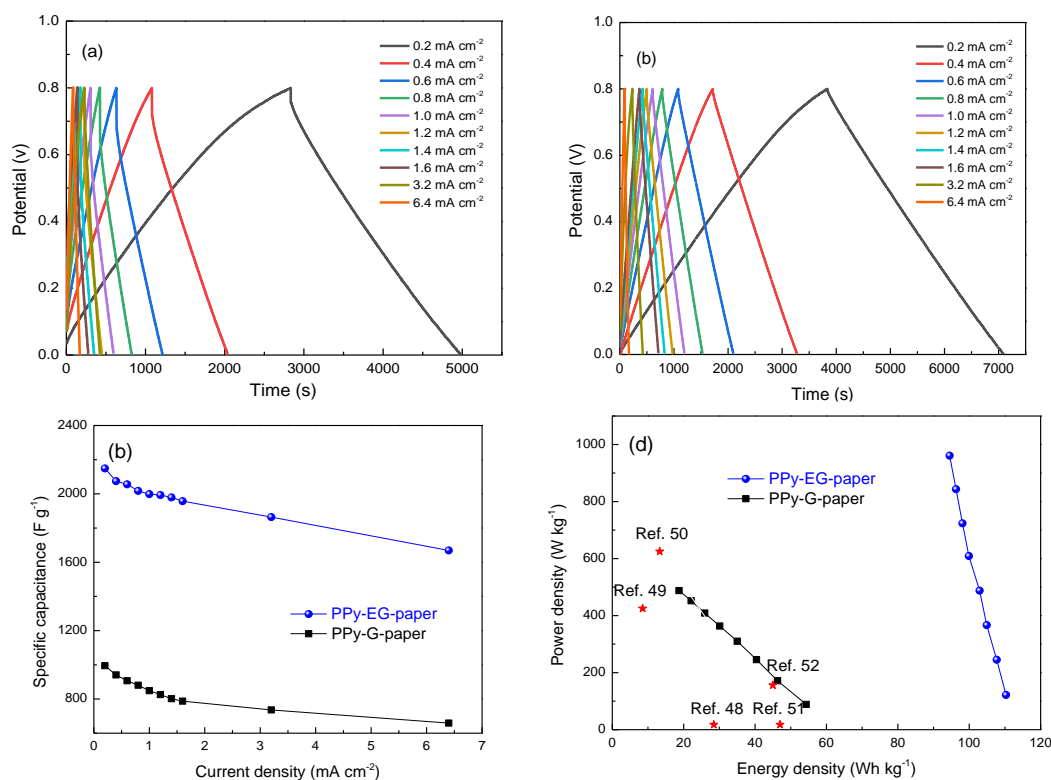


Figure 8. GCD curves of (a) PPY-G-paper and (b) PPY-EG-paper at different current densities; (c) specific capacitance of PPY-G-paper and PPY-EG-paper at different current densities; and (d) Ragone plots of PPY-G-paper and PPY-EG-paper.

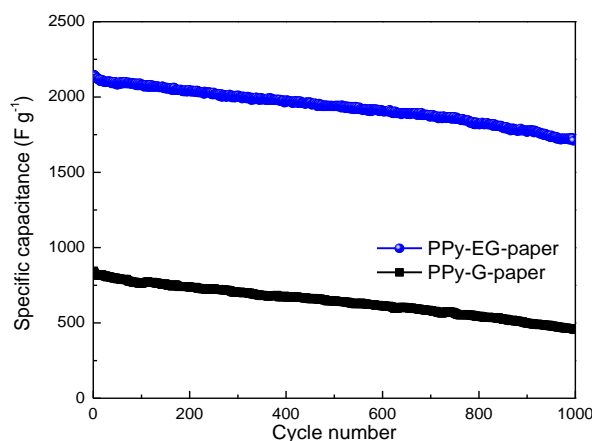


Figure 9. Cycling performance of PPY-G-paper and PPY-EG-paper at a current density of 0.8 mA·cm⁻².

4. Conclusions

In summary, we prepared the paper electrodes for supercapacitors with partially-exfoliated graphite and polypyrrole as the active materials. Graphite was coated on paper with pencil drawing and electrochemically exfoliated. PPY were deposited on the EG-paper through in situ polymerization. The as-prepared PPY-EG-paper exhibited remarkable electrochemical performance, in terms of a high specific capacitance of 2148 F·g⁻¹ at a current density of 0.8 mA·cm⁻², a high energy density of 110.3 Wh·kg⁻¹ at a power density of 121.9 W·kg⁻¹, favorable rate capability, and improved cycling life with retention of the initial specific capacitance at 80.4% after 1000 charge/discharge cycles. These results demonstrate the potential of PPY-EG-paper as a promising electrode for flexible supercapacitors.

Acknowledgments: This work was sponsored by the Scientific Innovation Team Project of the Education Department of Hubei Province (no. T201507), Wuhan Science and Technology Bureau (no. 2016010101010016), Natural Science Foundation of China (nos. 21673167 and 51703170), and the National Key Research and Development Program of China (no. 2016YFA0101102).

Author Contributions: Leping Huang and Weida Rao performed the experiments, analyzed the data, and interpreted the experimental results. Leping Huang and Jie Xu wrote the paper. Lingling Fan and Zikui Bai contributed to the experimental design. Weilin Xu, Haifeng Bao, and Jie Xu supervised the entire research progress.

Conflicts of Interest: The authors declare no conflict of interest.

References

1. Hu, L.; Pasta, M.; Mantia, F.L.; Cui, L.; Jeong, S.; Deshazer, H.D.; Choi, J.W.; Han, S.M.; Cui, Y. Stretchable, Porous, and Conductive Energy Textiles. *Nano Lett.* **2010**, *10*, 708–714. [[CrossRef](#)] [[PubMed](#)]
2. Shim, B.S.; Chen, W.; Doty, C.; Xu, C.; Kotov, N.A. Smart electronic yarns and wearable fabrics for human biomonitoring made by carbon nanotube coating with polyelectrolytes. *Nano Lett.* **2008**, *8*, 4151–4157. [[CrossRef](#)] [[PubMed](#)]
3. Hu, L.; Wu, H.; Mantia, F.L.; Yang, Y.; Cui, Y. Thin, Flexible Secondary Li-Ion Paper Batteries. *ACS Nano* **2010**, *10*, 5843–5848. [[CrossRef](#)] [[PubMed](#)]
4. Yuan, C.; Hou, L.; Li, D.; Shen, L.; Zhang, F.; Zhang, X. Synthesis of flexible and porous cobalt hydroxide/conductive cotton textile sheet and its application in electrochemical capacitors. *Electrochim. Acta* **2011**, *56*, 6683–6687. [[CrossRef](#)]
5. Liu, W.-W.; Yan, X.-B.; Lang, J.-W.; Peng, C.; Xue, Q.-J. Flexible and conductive nanocomposite electrode based on graphene sheets and cotton cloth for supercapacitor. *J. Mater. Chem.* **2012**, *22*, 17245–17253. [[CrossRef](#)]
6. Yao, B.; Jing, Z.; Kou, T.; Yu, S.; Liu, T.; Li, Y. Paper-based Electrodes for Flexible Energy Storage Devices. *Adv. Sci.* **2017**, *4*, 1700107. [[CrossRef](#)] [[PubMed](#)]
7. Cai, X.; Peng, M.; Yu, X.; Fu, Y.; Zou, D. Flexible planar/fiber-architected supercapacitors for wearable energy storage. *J. Mater. Chem. C* **2014**, *2*, 1184–1200. [[CrossRef](#)]
8. Jost, K.; Dion, G.; Gogotsi, Y. Textile energy storage in perspective. *J. Mater. Chem. A* **2014**, *2*, 10776–10787. [[CrossRef](#)]
9. Simon, P.; Gogotsi, Y.; Dunn, B. Where Do Batteries End and Supercapacitors Begin? *Science* **2014**, *343*, 1210–1211. [[CrossRef](#)] [[PubMed](#)]
10. Ramya, R.; Sivasubramanian, R.; Sangaranarayanan, M.V. Conducting polymers-based Electrochemical Supercapacitors-Progress and Prospects. *Electrochim. Acta* **2013**, *101*, 109–129. [[CrossRef](#)]
11. Wang, X.; Deng, J.; Duan, X.; Liu, D.; Liu, P. Fluorescent brightener CBS-X doped polypyrrole as smart electrode material for supercapacitors. *Appl. Energy* **2015**, *153*, 70–77. [[CrossRef](#)]
12. Xu, J.; Zhu, L.; Bai, Z.; Liang, G.; Liu, L.; Fang, D.; Xu, W. Conductive polypyrrole-bacterial cellulose nanocomposite membranes as flexible supercapacitor electrode. *Org. Electron.* **2013**, *14*, 3331–3338. [[CrossRef](#)]
13. Liang, G.; Zhu, L.; Xu, J.; Fang, D.; Bai, Z.; Xu, W. Investigations of poly(pyrrole)-coated cotton fabrics prepared in blends of anionic and cationic surfactants as flexible electrode. *Electrochim. Acta* **2013**, *103*, 9–14. [[CrossRef](#)]
14. Zhu, L.; Wu, L.; Sun, Y.; Li, M.; Xu, J.; Bai, Z.; Liang, G.; Liu, L.; Fang, D.; Xu, W. Cotton fabrics coated with lignosulfonate-doped polypyrrole for flexible supercapacitor electrodes. *RSC Adv.* **2014**, *4*, 6261–6266. [[CrossRef](#)]
15. Xu, J.; Wang, D.; Yuan, Y.; Wei, W.; Gu, S.; Liu, R.; Wang, X.; Liu, L.; Xu, W. Polypyrrole-coated cotton fabrics for flexible supercapacitor electrodes prepared using CuO nanoparticles as template. *Cellulose* **2015**, *22*, 1355–1363. [[CrossRef](#)]
16. Xu, J.; Wang, D.; Yuan, Y.; Wei, W.; Duan, L.; Wang, L.; Bao, H.; Xu, W. Polypyrrole/reduced graphene oxide coated fabric electrodes for supercapacitor application. *Org. Electron.* **2015**, *24*, 153–159. [[CrossRef](#)]
17. Xu, J.; Wang, D.; Fan, L.; Yuan, Y.; Wei, W.; Liu, R.; Gu, S.; Xu, W. Fabric electrodes coated with polypyrrole nanorods for flexible supercapacitor application prepared via a reactive self-degraded template. *Org. Electron.* **2015**, *26*, 292–299. [[CrossRef](#)]
18. Gholami, M.; Nia, P.M.; Alias, Y. Morphology and electrical properties of electrochemically synthesized pyrrole-formyl pyrrole copolymer. *Appl. Surf. Sci.* **2015**, *357*, 806–813. [[CrossRef](#)]

19. Huang, Y.; Li, H.; Wang, Z.; Zhu, M.; Pei, Z.; Xue, Q.; Huang, Y.; Zhi, C. Nanostructured Polypyrrole as a flexible electrode material of supercapacitor. *Nano Energy* **2016**, *22*, 422–438. [[CrossRef](#)]
20. Wang, Z.L.; He, X.J.; Ye, S.H.; Tong, Y.X.; Li, G.R. Design of Polypyrrole/Polyaniline Double-Walled Nanotube Arrays for Electrochemical Energy Storage. *ACS Appl. Mater. Interfaces* **2014**, *6*, 642–647. [[CrossRef](#)] [[PubMed](#)]
21. Peng, S.; Fan, L.; Wei, C.; Bao, H.; Zhang, H.; Xu, W.; Xu, J. Polypyrrole/nickel sulfide/bacterial cellulose nanofibrous composite membranes for flexible supercapacitor electrodes. *Cellulose* **2016**, *23*, 2639–2651. [[CrossRef](#)]
22. Liu, T.; Finn, L.; Yu, M.; Wang, H.; Zhai, T.; Lu, X.; Tong, Y.; Li, Y. Polyaniline and Polypyrrole Pseudocapacitor Electrodes with Excellent Cycling Stability. *Nano Lett.* **2014**, *14*, 2522–2527. [[CrossRef](#)] [[PubMed](#)]
23. Song, Y.; Liu, T.-Y.; Xu, X.-X.; Feng, D.-Y.; Li, Y.; Liu, X.-X. Pushing the Cycling Stability Limit of Polypyrrole for Supercapacitors. *Adv. Funct. Mater.* **2015**, *25*, 4626–4632. [[CrossRef](#)]
24. Liu, Y.; Wang, H.; Zhou, J.; Bian, L.; Zhu, E.; Hai, J.; Tang, J.; Tang, W. Graphene/polypyrrole intercalating nanocomposites as supercapacitors electrode. *Electrochim. Acta* **2013**, *112*, 44–52. [[CrossRef](#)]
25. Fu, H.; Du, Z.J.; Zou, W.; Li, H.Q.; Zhang, C. Carbon nanotube reinforced polypyrrole nanowire network as a high-performance supercapacitor electrode. *J. Mater. Chem. A* **2013**, *1*, 14943–14950. [[CrossRef](#)]
26. Shi, K.; Zhitomirsky, I. Influence of current collector on capacitive behavior and cycling stability of Tiron doped polypyrrole electrodes. *J. Power Sources* **2013**, *240*, 42–49. [[CrossRef](#)]
27. Chen, S.; Zhitomirsky, I. Polypyrrole electrodes doped with sulfanilic acid azochromotop for electrochemical supercapacitors. *J. Power Sources* **2013**, *243*, 865–871. [[CrossRef](#)]
28. Liu, S.; Yu, T.; Wu, Y.; Li, W.; Li, B. Evolution of cellulose into flexible conductive green electronics: A smart strategy to fabricate sustainable electrodes for supercapacitors. *RSC Adv.* **2014**, *4*, 34134–34143. [[CrossRef](#)]
29. Zheng, G.; Hu, L.; Wu, H.; Xie, X.; Cui, Y. Paper supercapacitors by a solvent-free drawing method. *Energy Environ. Sci.* **2011**, *4*, 3368–3373. [[CrossRef](#)]
30. Tao, J.; Ma, W.; Liu, N.; Ren, X.; Shi, Y.; Su, J.; Gao, Y. High-Performance Solid-State Supercapacitors Fabricated by Pencil Drawing and Polypyrrole Depositing on Paper Substrate. *Nano-Micro Lett.* **2015**, *7*, 276–281. [[CrossRef](#)]
31. Song, Y.; Feng, D.Y.; Liu, T.Y.; Li, Y.; Liu, X.X. Controlled partial-exfoliation of graphite foil and integration with MnO₂ nanosheets for electrochemical capacitors. *Nanoscale* **2015**, *7*, 3581–3587. [[CrossRef](#)] [[PubMed](#)]
32. Down, M.P.; Foster, C.W.; Ji, X.; Banks, C.E. Pencil drawn paper based supercapacitors. *RSC Adv.* **2016**, *6*, 81130–81141. [[CrossRef](#)]
33. Bernalte, E.; Foster, C.W.; Brownson, D.A.C.; Mosna, M.; Smith, G.C.; Banks, C.E. Pencil It in: Exploring the Feasibility of Hand-Drawn Pencil Electrochemical Sensors and Their Direct Comparison to Screen-Printed Electrodes. *Biosensors* **2016**, *6*, 45. [[CrossRef](#)] [[PubMed](#)]
34. Song, Y.; Xu, J.L.; Liu, X.X. Electrochemical anchoring of dual doping polypyrrole on graphene sheets partially exfoliated from graphite foil for high-performance supercapacitor electrode. *J. Power Sources* **2014**, *249*, 48–58. [[CrossRef](#)]
35. Nyström, G.; Razaq, A.; Strømme, M.; Nyholm, L.; Mihranyan, A. Ultrafast All-Polymer Paper-Based Batteries. *Nano Lett.* **2009**, *9*, 3635–3639. [[CrossRef](#)] [[PubMed](#)]
36. Li, S.; Huang, D.; Yang, J.; Zhang, B.; Zhang, X.; Yang, G.; Wang, M.; Shen, Y. Freestanding bacterial cellulose-polypyrrole nanofibres paper electrodes for advanced energy storage devices. *Nano Energy* **2014**, *9*, 309–317. [[CrossRef](#)]
37. Wang, D.; Li, Y.X.; Shi, Z.; Qin, H.L.; Wang, L.; Pei, X.F.; Jin, J. Spontaneous Growth of Free-Standing Polypyrrole Films at an Air/Ionic Liquid Interface. *Langmuir* **2010**, *26*, 14405–14408. [[CrossRef](#)] [[PubMed](#)]
38. Zhu, L.; Zhang, L.; Wu, L.; Sun, Y.; Bai, Z.; Xu, J.; Liang, G.; Xu, W. Conductive Cotton Fabrics for Heat Generation Prepared by Mist Polymerization. *Fibers Polym.* **2014**, *15*, 1804–1809. [[CrossRef](#)]
39. Xu, Q.; Fan, L.; Yuan, Y.; Wei, C.; Bai, Z.; Xu, J. All-solid-state yarn supercapacitors based on hierarchically structured bacterial cellulose nanofiber-coated cotton yarns. *Cellulose* **2016**, *23*, 3987–3997. [[CrossRef](#)]
40. Yan, D.; Liu, Y.; Li, Y.; Zhuo, R.; Wu, Z.; Ren, P.; Li, S.; Wang, J.; Yan, P.; Geng, Z. Synthesis and electrochemical properties of MnO₂/rGO/PEDOT:PSS ternary composite electrode material for supercapacitors. *Mater. Lett.* **2014**, *127*, 53–55. [[CrossRef](#)]
41. Wang, Z.-L.; Guo, R.; Li, G.-R.; Lu, H.-L.; Liu, Z.-Q.; Xiao, F.-M.; Zhang, M.; Tong, Y.-X. Polyaniline nanotube arrays as high-performance flexible electrodes for electrochemical energy storage devices. *J. Mater. Chem.* **2012**, *22*, 2401–2404. [[CrossRef](#)]

42. Feng, J.X.; Li, Q.; Lu, X.F.; Tong, Y.X.; Li, G.R. Flexible symmetrical planar supercapacitors based on multi-layered MnO₂/Ni/graphite/paper electrodes with high-efficient electrochemical energy storage. *J. Mater. Chem. A* **2014**, *2*, 2985–2992. [[CrossRef](#)]
43. Feng, J.X.; Ye, S.H.; Lu, X.F.; Tong, Y.X.; Li, G.R. Asymmetric Paper Supercapacitor Based on Amorphous Porous Mn₃O₄ Negative Electrode and Ni(OH)₂ Positive Electrode: A Novel and High-Performance Flexible Electrochemical Energy Storage Device. *ACS Appl. Mater. Interfaces* **2015**, *7*, 11444–11451. [[CrossRef](#)] [[PubMed](#)]
44. Devarayan, K.; Lei, D.; Kim, H.Y.; Kim, B.S. Flexible transparent electrode based on PANi nanowire/nylon nanofiber reinforced cellulose acetate thin film as supercapacitor. *Chem. Eng. J.* **2015**, *273*, 603–609. [[CrossRef](#)]
45. Gui, Z.; Zhu, H.; Gillette, E.; Han, X.; Rubloff, G.W.; Hu, L.; Sang, B.L. Natural Cellulose Fiber as Substrate for Supercapacitor. *ACS Nano* **2013**, *7*, 6037–6046. [[CrossRef](#)] [[PubMed](#)]
46. Qian, J.; Jin, H.; Chen, B.; Lin, M.; Lu, W.; Tang, W.M.; Xiong, W.; Chan, L.W.; Lau, S.P.; Yuan, J. Aqueous manganese dioxide ink for paper-based capacitive energy storage devices. *Angew. Chem. Int. Ed.* **2015**, *54*, 6800–6803. [[CrossRef](#)] [[PubMed](#)]
47. Yuan, L.; Yao, B.; Hu, B.; Huo, K.; Chen, W.; Zhou, J. Polypyrrole-coated paper for flexible solid-state energy storage. *Energy Environ. Sci.* **2013**, *6*, 470–476. [[CrossRef](#)]
48. Yuan, L.; Xiao, X.; Ding, T.; Zhong, J.; Zhang, X.; Shen, Y.; Hu, B.; Huang, Y.; Zhou, J.; Wang, Z.L. Paper-based supercapacitors for self-powered nanosystems. *Angew. Chem. Int. Ed.* **2012**, *51*, 4934–4938. [[CrossRef](#)] [[PubMed](#)]
49. Kang, Y.R.; Li, Y.L.; Hou, F.; Wen, Y.Y.; Su, D. Fabrication of electric papers of graphene nanosheet shelled cellulose fibres by dispersion and infiltration as flexible electrodes for energy storage. *Nanoscale* **2012**, *4*, 3248–3253. [[CrossRef](#)] [[PubMed](#)]
50. Akhter, T.; Islam, M.M.; Faisal, S.N.; Haque, E.; Minett, A.I.; Liu, H.K.; Konstantinov, K.; Dou, S. Self-assembled N/S co-doped Flexible Graphene Paper for High Performance Energy Storage and Oxygen Reduction Reaction. *ACS Appl. Mater. Interfaces* **2016**, *8*, 2078–2087. [[CrossRef](#)] [[PubMed](#)]
51. Perera, S.D.; Rudolph, M.; Mariano, R.G.; Nijem, N.; Ferraris, J.P.; Chabal, Y.J., Jr.; Balkus, K.J. Manganese oxide nanorod-graphene/vanadium oxide nanowire-graphene binder-free paper electrodes for metal oxide hybrid supercapacitors. *Nano Energy* **2013**, *2*, 966–975. [[CrossRef](#)]
52. Foo, C.Y.; Sumboja, A.; Tan, D.J.H.; Wang, J.; Lee, P.S. Flexible and Highly Scalable V₂O₅-rGO Electrodes in an Organic Electrolyte for Supercapacitor Devices. *Adv. Energy Mater.* **2014**, *4*, 1400236. [[CrossRef](#)]
53. Kong, L.; Zhang, C.; Wang, J.; Qiao, W.; Ling, L.; Long, D. Free-Standing T-Nb₂O₅/Graphene Composite Papers with Ultrahigh Gravimetric/Volumetric Capacitance for Li-Ion Intercalation Pseudocapacitor. *ACS Nano* **2015**, *9*, 11200–11208. [[CrossRef](#)] [[PubMed](#)]
54. Ghosh, A.; Ra, E.J.; Jin, M.; Jeong, H.K.; Kim, T.H.; Biswas, C.; Lee, Y.H. High Pseudocapacitance from Ultrathin V₂O₅ Films Electrodeposited on Self-Standing Carbon-Nanofiber Paper. *Adv. Funct. Mater.* **2011**, *21*, 2541–2547. [[CrossRef](#)]
55. Hu, S.; Rajamani, R.; Yu, X. Flexible solid-state paper based carbon nanotube supercapacitor. *Appl. Phys. Lett.* **2012**, *100*, 104103–104104. [[CrossRef](#)]

